

Four-copper complexes in Si and the Cu-photoluminescence defect: A first-principles study

A. Carvalho*

Department of Physics, I3N, University of Aveiro, Campus Universitário de Santiago, 3810-193 Aveiro, Portugal

D. J. Backlund and S. K. Estreicher

Department of Physics, Texas Tech University, Lubbock, Texas 79409-1051, USA

(Received 6 July 2011; revised manuscript received 27 September 2011; published 31 October 2011)

Complexes containing four Cu impurities in Si are systematically investigated using density functional theory. The complexes include various combinations of substitutional and interstitial copper. The structures, formation and binding energies, approximate gap levels, and vibrational spectra are calculated and the results compared to the measured properties of the Cu_{PL} defect. The best candidate out of those investigated is the $\text{Cu}_{\text{s}1}\text{Cu}_{\text{i}3}$ complex recently proposed by Shirai *et al.* [*J. Phys: Condens. Matter* **21**, 064249 (2009)]. The estimated positions of the gap levels of $\text{Cu}_{\text{s}1}\text{Cu}_{\text{i}n}$, with $n = 0, \dots, 3$, suggest a straightforward explanation as to why only the defects Cu_{s} and $\text{Cu}_{\text{s}1}\text{Cu}_{\text{i}3}$ occur in high-resistivity material.

DOI: 10.1103/PhysRevB.84.155322

PACS number(s): 71.55.Ak, 88.40.jj, 61.72.J-, 78.55.Ap

I. INTRODUCTION

Copper is a common contaminant in both electronic-grade and photovoltaic Si. It is often present in the as-grown material in the case of multicrystalline solar cells, which are increasingly obtained from low-cost “solar-grade” feedstock with a high-impurity content, including transition-metal impurities.^{1,2} Copper is also accidentally introduced during the various processing steps involved in the fabrication of photovoltaic or electronic devices.

Isolated interstitial copper (Cu_{i}) has a minor impact on the carrier lifetime. It has a donor level at $E_{\text{c}} - 0.15$ eV,^{3,4} and is therefore in the positive charge state in *p*-type and high-resistivity Si. However, Cu_{i} is the fastest-diffusing transition-metal impurity, migrating among tetrahedral interstitial (T) sites with an activation energy of only 0.18 eV.⁵⁻⁷ As a result, copper rapidly forms electrically active precipitates at dislocations and grain boundaries, as well as silicides in *n*-type Si.^{1,8-13}

If Cu_{i} encounters a preexisting vacancy, it becomes substitutional (Cu_{s}) with a calculated gain in energy of 3.13 eV, which is considerably less than the formation energy of the vacancy 3.85 eV (both values for the neutral charge state, at the present level of theory). Thus, the concentration of Cu_{s} at moderate temperatures is always very much smaller than that of Cu_{i} and depends on the presence of isolated vacancies, that is, on the history of the sample.

Substitutional copper overlaps covalently with the four Si dangling bonds and the energy gained by the formation of these four weak Cu-Si bonds is the reason for the energy gain in the reaction $\text{Cu}_{\text{i}} + \text{V} \rightarrow \text{Cu}_{\text{s}}$. However, this results in the appearance of several new levels in the gap. According to deep-level transient spectroscopy (DLTS) and minority carrier transient spectroscopy (MCTS) measurements, Cu_{s} has donor and acceptor levels at $E_{\text{v}} + 0.20$ – 0.23 eV and $E_{\text{v}} + 0.42$ – 0.46 eV, respectively, and maybe a double-acceptor level at $E_{\text{c}} - 0.16$ eV.¹⁴⁻¹⁷ The identification of the donor and first-acceptor levels as being due to Cu_{s} has been corroborated by recent data revealing details about the interaction of Cu with the A center (VO).¹⁸ The DLTS peak at $E_{\text{c}} - 0.16$ eV that has been associated with a double-acceptor level of Cu_{s} has

also been assigned to the donor level of Cu_{i} .⁴ However, it is also possible that the donor level of Cu_{i} and a double-acceptor level of Cu_{s} are close to each other. In any case, Cu_{s} is in the positive charge state in *p*-type Si, in the negative charge state in high-resistivity Si, and moderately doped in *n*-type Si, and in the negative or maybe double-negative charge state in *n*-type Si.

A Cu-related photoluminescence (PL) defects has been detected following either Cu implantation or Cu in-diffusion from a metallic source at a few hundred degrees Celsius, followed by an anneal (typically ~ 700 °C) and a rapid quench.¹⁹ Such studies have only been reported for high-resistivity Si, probably to limit problems associated with free-carrier absorption. The defect related with the intense PL band with a sharp zero-phonon line at 1014 eV is the subject of this paper.

This band, first reported by Minaev *et al.*,²⁰ was shown to be Cu related by Weber *et al.*^{19,21} We label the associated defect Cu_{PL} . It has been correlated with a DLTS donor level at $E_{\text{v}} + 0.10$ eV.²² For many years, Cu_{PL} was believed to be a substitutional-interstitial $\text{Cu}_{\text{s}}\text{Cu}_{\text{i}}$ pair, as proposed by Weber *et al.*¹⁹ Theoretical studies confirmed that this pair has indeed some of the key features of Cu_{PL} .^{23,24}

However, PL studies in isotopically pure ²⁸Si samples with various combinations of Cu isotopes have demonstrated that Cu_{PL} contains not two, but at least four, Cu atoms.²⁵ Indeed, the sensitivity of PL experiments in isotopically pure Si samples increases by about two orders of magnitude relative to the same experiments in ^{nat}Si. Stegner *et al.* also identified an entire family of apparently similar PL centers including various combinations of Cu, Ag, Au, Li, and other metallic impurities, all of them containing “at least four,” and in a few cases, “at least five,” metallic impurities.^{25,26} No defect containing two or three metallic impurities is visible in the PL spectra.

Although experimentally it could not be proven that the defect contains no more than four atoms, since one (or more) metal impurity could be invisible to PL in the case of the trigonal Cu_{PL} , the fact that four atoms have been invariably detected in similar PL centers containing Ag or Au atoms suggests that there are exactly four atoms in all of those defects,

as it is unlikely that a fifth (or sixth) impurity always remains invisible to PL when the atomic composition and symmetry of the defect change.

The key observed properties of the Cu_{PL} defect can be summarized as follows.

(1) Cu_{PL} gives rise to an intense PL emission at 1.014 eV, with the high radiative intensity and zero phonon line (ZPL) external field splitting characteristics of an isoelectronic center.¹⁹ The defect is donorlike, with a tightly bound hole and Coulomb-bound electron.

(2) The PL band has been correlated with a DLTS level at $E_v + 0.10$ eV.²² The absence of the Pool-Frenkel emission enhancement rules out the acceptor nature of the center and the purely ionic (polar) type of bonding. The polarization potential describing an emission from a neutral impurity gave a satisfactory fit to the experimental data.²⁷ Thus, Cu_{PL} has one donor level at $E_c + 0.10$ eV. No acceptor level has been detected.

(3) The PL band exhibits sharp phonon sidebands separated by 7.05 meV, which exhibit a small shift with the Cu isotope.^{19,20,25} These sidebands are indicative of a Cu-related pseudolocal vibrational mode (pLVM) at 56 cm^{-1} . Much weaker sidebands occur at 16.4 and 25.1 meV (132 and 202 cm^{-1} , respectively).

(4) Uniaxial stress and Zeeman data show that the center is trigonal.^{19,21}

(5) The thermal dissociation energy of the DLTS Cu_{PL} -related center has been measured to be 1.02 eV in *p*-type Si.²⁷ Since the migration barrier of Cu_i is 0.18 eV, the binding energy is approximately 0.84 eV. Note that the dissociation energy obtained from the analysis of the PL annealing in another study gave a 0.63-eV activation energy²⁸ and the formation of the Cu_{PL} center was estimated to be 0.57 eV based on an analysis of the PL intensity.^{28,29}

(6) The Cu_{PL} defect dissociates following a 30-min anneal at 250°C , and the amplitude of the DLTS peaks associated with Cu_s increases.^{30,31} If Cu is reintroduced into the sample, Cu_{PL} reappears. Thus, the core of Cu_{PL} must be or include, Cu_s .

(7) Cu_{PL} forms following implantation or in-diffusion. The in-diffusion of Cu from a metallic source must be followed by an anneal [above 400°C , optimal at 700°C (Ref. 31)]. The concentration of this center is estimated to be less than 0.1% of the equilibrium copper solubility at the diffusion temperature.¹⁷ Note that our calculations give

$$\text{Cu}_i^0 + \text{V}^0 \rightarrow \text{Cu}_s^0 + 3.13\text{ eV}, \quad (1)$$

while we obtain a formation energy of 3.85 eV for the vacancy. Assuming that no vacancies are present in the material, the overall energy balance is 0.72 eV, and at 700°C , this leads to a Boltzmann factor $\exp\{-0.72\text{ eV}/k_B T\} \sim 0.02\%$.

Two structures containing four Cu atoms have been discussed as the Cu_{PL} defect. Shirai *et al.* proposed a trigonal defect consisting of one substitutional and three interstitial copper atoms ($\text{Cu}_{s1}\text{Cu}_{i3}$).³² However, the gap levels of the complex and its vibrational spectrum have not been calculated. Nakamura *et al.*³³ proposed instead that the core of the defect is copper at the bond-centered (BC) site (Cu_{BC}),^{34,35} and that Cu_{PL} is a trigonal $\text{Cu}_{\text{BC}}\text{Cu}_{i3}$ complex. No theoretical support

for this structure based on its electrical or optical properties was provided. Further, the previous studies have not explained why Cu_4 clusters are observed, while the simpler Cu_2 and Cu_3 or larger Cu_5 clusters are not detected.

In this paper, we consider a variety of *a priori* possible combinations of four-Cu complexes in Si combining substitutional and interstitial Cu atoms, including Cu_{BC} . The structures, formation and binding energies, and approximate gap levels are calculated. Several configurations can be eliminated as plausible candidates as the Cu_{PL} defect. The vibrational spectra of the remaining defect centers are calculated. The properties of the most stable structures are compared to the experimental data. The sequence of gap levels of the $\text{Cu}_{s1}\text{Cu}_{in}$ defects with $n = 0, \dots, 3$ suggests a reason why only Cu_s and $\text{Cu}_{s1}\text{Cu}_{i3}$ are observed. The level of theory is described in Sec. II. The results of the calculations are in Sec. III, and the key points are discussed in Sec. IV.

II. METHODOLOGY

The calculations are performed using density functional theory. The electronic core is accounted for by using *ab initio* norm-conserving pseudopotentials with the Troullier-Martins parametrization³⁶ in the Kleinman-Bylander form.³⁷ The electronic valence regions are treated self-consistently within density functional theory,³⁸ as implemented in the SIESTA package.^{39,40} The generalized gradient approximation of Perdew, Burke, and Ernzerhof is used for the exchange-correlation functional.⁴¹

The basis sets for the Kohn-Sham states are linear combinations of numerical atomic orbitals.^{42,43} These are double-zeta-polarized basis sets, including two sets of *s* and *p* and one set of *d* functions for Si and two sets of *s* and *d* functions for Cu. The valence electrons and semicore Cu 3*d* electrons are treated explicitly. The charge density is projected on a real-space grid with an equivalent cutoff energy of 250 Ry to calculate the exchange-correlation and Hartree potentials. The nuclei are treated classically, and their positions optimized using a conjugate gradient algorithm.^{39,40}

The host crystal is represented by a 216-atom supercell (Si_{216}). The lattice constant of the supercell is optimized in each charge state. A Monkhorst-Pack⁴⁴ (MP) scheme is used to sample the Brillouin zone. Convergence tests were performed for Cu_i , Cu_s , Cu_iCu_s , and Cu_sCu_s defects. These showed that the geometry is already fully converged ($< 10^{-3}$ nm) for Γ -point calculations. First donor and acceptor levels are also already converged within 0.11 eV for Γ -point calculations, with the exception of the donor level of Cu_i , which can be only calculated with accuracy using MP-2³ sampling. For that *k*-point sampling density, the calculated level differs only 0.07 eV from that obtained in a MP-4³ calculation. These results show that MP-2³ sampling is reasonably accurate for the calculation of the electronic levels of defects in a 216-atom supercell. Thus, we used for the geometry optimization and total energy calculations MP-2^{3,2} sampling, whereas for the force constant, calculations are performed at the Γ point.

The dynamical matrices are obtained from a direct calculation of the force-constant matrix. The eigenvalues ω_s ($s = 1, 2, \dots, 3N$, where N is the number of atoms) are the

normal-mode frequencies of the system and the orthonormal eigenvectors $e_{\alpha i}^s$ (where α numbers the nuclei and $i = x, y, z$) give the relative displacements of all the nuclei for every normal mode s . The localization of the mode s on the defect D is defined as

$$L_D^2 = \sum_i \sum_{\alpha \in D} (e_{\alpha i}^s)^2$$

and the sum runs over all the atoms belonging to the defect D (or over a set of atoms D in the defect).

The ionization levels are calculated by comparing the ionization energies and electron affinities of the supercells containing the defects with those of perfect supercells (marker method).⁴⁵ Using the energy of bulk supercells when a hole is added to the top of the valence band or an electron to the bottom of the conduction band, it is possible to place defect acceptor and donor levels with respect to the conduction and valence bands, respectively. The method works best for deep levels that are not too far from the band used as a reference. This is due in one instance to the band-gap underestimation error, the effect of which increases with the distance separating the level from the reference band, but practically cancels out when this distance is small. On the other hand, levels very close to the reference band edge are often very delocalized and therefore more affected by spurious defect-defect interactions.

At $T = 0$ K, the formation energy of a neutral defect is defined as

$$E_f(D) = E(\text{Si}_{216} : D) - n_{\text{Cu}}\mu_{\text{Cu}} - n_{\text{Si}}\mu_{\text{Si}},$$

where $E(\text{Si}_{216} : D)$ is the total energy of the supercell with a defect D , n_{Cu} and n_{Si} are the number of Cu and Si atoms it contains, and μ_{Cu} and μ_{Si} are the respective chemical potentials. The chemical potentials reflect the availability of the chemical species. Here, they are taken to be the energy per atom in bulk Si and bulk Cu reservoirs. The formation energy of charged defects was obtained from the formation energy of the neutral charge state using the ionization levels calculated with the marker method as

$$E_f(D^q) = E_f(D^{q-1}) + e[\mu_e - E(q/q + 1)],$$

where e is the electron charge and μ_e its chemical potential (at $T = 0$, the Fermi level).

III. FOUR-COPPER COMPLEXES

Interstitial copper is the most stable form of this impurity in silicon. In the neutral charge state, its formation energy is 1.58 eV, or 0.72 eV lower than that of neutral substitutional copper. However, if a vacancy is provided, interstitial copper becomes substitutional through the reaction in Eq. (1). The 3.13-eV energy gain is less than the formation energy of the vacancy, which is 3.85 eV at the current level of theory. If there is Cu contamination in the melt, this reaction can occur during crystal growth, leaving some copper atoms occupying substitutional lattice positions. If Cu is implanted into the crystal, some vacancies will result from the implantation. If Cu is diffused into the crystal, an annealing step at a relatively high temperature can also result in the formation of Cu_s . In any case, the concentration of Cu_s depends on the history of the

TABLE I. Ionization levels (eV) of substitutional and interstitial copper. Experimental values [for Cu_s (Refs. 14 and 16) and Cu_i (Ref. 4)] are listed in parentheses, below the respective calculated values. Note that the double-acceptor level of Cu_s has also been assigned to the single donor level of Cu_i (Ref. 4). The donor and acceptor levels are calculated with respect to the valence and conduction bands, respectively. When the opposite band edge is used for comparison with the experimental values, the calculated band gap $E_g = 0.78$ eV is used.

Defect	$E(+/0)$	$E(0/-)$	$E(-/=)$
Cu_i	$E_c - 0.09$ ($E_c - 0.15$)		
Cu_s	$E_v + 0.19$ ($E_v + 0.21-0.23$)	$E_v + 0.29$ ($E_v + 0.43-0.48$)	$E_c - 0.36$ ($E_c - 0.16-0.17$)

sample, not just on the total copper concentration. Since Cu_{PL} contains Cu_s , its concentration also depends on the history of the sample and on the way copper is introduced.

Cu_s is both a donor and an acceptor (Table I). The first-acceptor level is in the lower half of the band gap and, therefore, Cu_s is in the negative charge state in intrinsic material. Thus, Cu_s^- is a Coulomb trap for the much more abundant and highly mobile Cu_i^+ .⁵

A model for the interaction of the simplest copper defects (combinations of Cu_s and Cu_i) as they form small copper clusters and leading to the formation of the Cu_{PL} defect must provide a defect reaction chain that can occur at room temperature, and which culminates with the formation of a defect with four copper atoms, which is stable up to 250 °C.

We have investigated ten defects incorporating four copper atoms, m at substitutional sites and n at interstitial (T or BC) sites ($\text{Cu}_{sm}\text{Cu}_{in}$ with $m + n = 4$). They are Cu_{s4} , $\text{Cu}_{s3}\text{Cu}_{i1}$ (including two possible starting configurations with Cu_i at the T or BC sites), $\text{Cu}_{s2}\text{Cu}_{i2}$ (five possible configurations, but only one is trigonal), $\text{Cu}_{s1}\text{Cu}_{i3}$, and $\text{Cu}_{\text{BC}}\text{Cu}_{i3}$. Additionally, we have considered two defects containing a silicon self-interstitial, $\text{I}_{\text{Si}}\text{Cu}_s\text{Cu}_{s3}$ and $\text{I}_{\text{Si}}\text{Cu}_s\text{Cu}_{i3}$, which, as will be considered below, are obtained from the relaxation of the unstable $\text{Cu}_{\text{BC}}\text{Cu}_{s3}$ and $\text{Cu}_{\text{BC}}\text{Cu}_{i3}$ defects. We did not include a complex of four Cu_i 's since the long-range repulsion between Cu_i^+ 's makes its formation most unlikely. Further, the thermal dissociation of Cu_{PL} is known to leave Cu_s , and the reaction is reversible upon reintroduction of copper into the sample.³⁰

The formation energies versus Fermi level of selected $\text{Cu}_{sm}\text{Cu}_{in}$ defects are shown in Fig. 1. The ionization levels of the most stable of each $\text{Cu}_{sm}\text{Cu}_{in}$ defects are given in Table II. All but one of these 10 defects can be excluded as possible candidates as Cu_{PL} because they have low stability, or because of their electronic structure, gap levels, and/or vibrational spectra. We start by considering this evidence in Sec. III A. Then, Sec. III B is dedicated to the Cu_4 defect with the lowest formation energy amongst those investigated, $\text{Cu}_{s1}\text{Cu}_{i3}$. We compare its calculated properties to those of Cu_{PL} and discuss why $\text{Cu}_{s1}\text{Cu}_{i1}$, $\text{Cu}_{s1}\text{Cu}_{i2}$, and $\text{Cu}_{s1}\text{Cu}_{i4}$ are not observed.

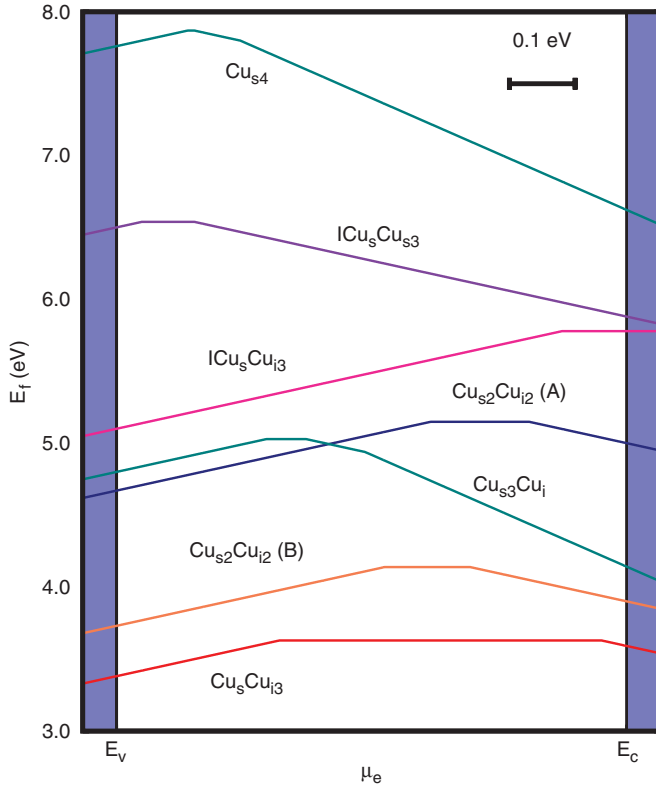


FIG. 1. (Color online) Formation energies of various $\text{Cu}_{sm}\text{Cu}_{in}$ defects as a function of the Fermi level (μ_e). The two structures that include $\text{I}_{\text{Si}}\text{Cu}_s$ are those that initiate with Cu_{BC} . Only the least (A) and the most stable of the $\text{Cu}_{s2}\text{Cu}_{i2}$ complexes (B) are shown.

A. Cu_4 complexes unlikely to be Cu_{PL}

1. Cu_{s4}

Four substitutional copper complexes (Cu_{s4}) can, in principle, exist. One possible trigonal configuration has an axial Cu_s with three nonaxial Cu_s nearest neighbors. However, the formation energy of the Cu_{s4} complex is the highest of all Cu_4 defects investigated here (Fig. 1), almost 2 eV per Cu atom. Further, this defect is highly unlikely to exhibit the observed annealing behavior at 250 °C: disappearance of Cu_{PL} leaving isolated Cu_s since each Cu_s is strongly bound. For these reasons, we conclude that Cu_{s4} is not a dominant defect in Si and is not the Cu_{PL} defect.

TABLE II. Ionization levels of the most stable $\text{Cu}_{sm}\text{Cu}_{in}$ defects. The position of a level very close to a band is especially unreliable since the associated wave function is artificially confined by the finite size of the supercell.

Defect	$E(0/+)$	$E(-/0)$
Cu_{s4}	$E_v + 0.11$	$E_c - 0.66$
$\text{I}_{\text{Si}}\text{Cu}_s\text{Cu}_{s3}$	$E_v + 0.04$	$E_c - 0.66$
$\text{I}_{\text{Si}}\text{Cu}_s\text{Cu}_{i3}$	$E_v + 0.68$	
$\text{Cu}_{s3}\text{Cu}_{i1}$	$E_v + 0.23$	$E_c - 0.49$
$\text{Cu}_{s2}\text{Cu}_{i2}$ (B)	$E_v + 0.41$	$E_c - 0.24$
$\text{Cu}_{s1}\text{Cu}_{i3}$	$E_v + 0.25$	$E_c - 0.04(?)$

2. $\text{Cu}_{s3}\text{Cu}_{i1}$

Another option that can be ruled out is $\text{Cu}_{s3}\text{Cu}_{i1}$. This defect could, in principle, form following the trapping of two interstitial copper atoms at a Cu_sCu_i pair if vacancies are available to bring the two Cu_i 's into substitutional sites. This defect has a donor level at $E_v + 0.23$ eV, not far from the electrical level of the Cu_{PL} defect. However, we note that it also has a deep acceptor level close to mid-gap. Therefore, it seems incompatible with the PL emission at 1.014 eV. Further, the formation energy of this defect is also quite high compared with other four-copper defects (Fig. 1).

3. Cu_{BC} and related defects

Isolated Cu_{BC} (Ref. 34) and then the $\text{Cu}_{\text{BC}}\text{Cu}_{i3}$ complex³³ have been proposed to be Cu_{PL} . However, in contrast to interstitial hydrogen, interstitial copper is not stable at the bond-centered site in Si. Indeed, Cu makes much longer bonds with Si than H does and there is simply not enough space available at the BC for it to become a local minimum of the potential energy. If forced into this site with its two Si nearest neighbors relaxed all the way to the plane of their nearest neighbors, Cu moves to the substitutional site and expels a Si self-interstitial, forming a configuration we label $\text{I}_{\text{Si}}\text{Cu}_s$. This configuration is 1.97 eV higher in energy than Cu_i (in the positive charge state).

Similarly, $\text{Cu}_{\text{BC}}\text{Cu}_{i3}$ spontaneously relaxes to $\text{I}_{\text{Si}}\text{Cu}_s\text{Cu}_{i3}$ (Fig. 2). This structure is trigonal, but its formation energy (Fig. 1) is almost 2 eV higher than that of the much simpler $\text{Cu}_s\text{Cu}_{i3}$ complex. Further, it has a deep donor level high in the gap (and no acceptor level), while the Cu_{PL} center has a donor level at $E_v + 0.10$ eV. Thus, $\text{I}_{\text{Si}}\text{Cu}_s\text{Cu}_{i3}$ is not a possible candidate for Cu_{PL} .

For completeness, we have also considered a model constituted by a bond-centered copper decorated with three substitutional copper atoms $\text{Cu}_{\text{BC}}\text{Cu}_{s3}$. It is also unstable and relaxes to $\text{I}_{\text{Si}}\text{Cu}_s\text{Cu}_{s3}$. Its formation energy (Fig. 1) is even higher than that of $\text{I}_{\text{Si}}\text{Cu}_s\text{Cu}_{i3}$. Thus, our calculations firmly rule out the existence of Cu_{BC} either as an isolated interstitial or as a component of a four-copper complex.

4. $\text{Cu}_{s2}\text{Cu}_{i2}$ defects

A more realistic model incorporates two interstitial and two substitutional copper atoms, $\text{Cu}_{s2}\text{Cu}_{i2}$. An obvious trigonal configuration has $\text{Cu}_i \dots \text{Cu}_s - \text{Cu}_s \dots \text{Cu}_i$ aligned along the same trigonal axis [Fig. 3(a)]. This structure resembles two Cu_sCu_i pairs facing each other. The formation mechanism relies on the formation of a Cu_sCu_s core, which, if it exhibits an acceptor level in the lower half of the gap, traps two Cu_i 's.

Next-neighbor Cu_s - Cu_s pairs (Cu_{s2}) have a lower formation energy per copper atom than Cu_s . Indeed, in the neutral charge state, the formation energy of the vacancy is 3.85 eV and that of the divacancy 5.64 eV. If we assume a preexisting V_2 , the reactions $\text{Cu}_i + \text{V}_2 \rightarrow \{\text{VCuV}\}$ and $\text{Cu}_i + \{\text{VCuV}\} \rightarrow \text{Cu}_{s2}$, where VCuV represents a defect with Cu in the divacancy cage, release 3.4 and 2.2 eV, respectively, in the neutral charge state.⁴⁶ Two nearby Cu_i 's could therefore, in principle, produce a small amount of Cu_{s2} defects, but the presence of Cu_i^+ in the immediate vicinity of another Cu_i^+ is unlikely. Therefore, the reactions leading to the formation of Cu_{s2} require some

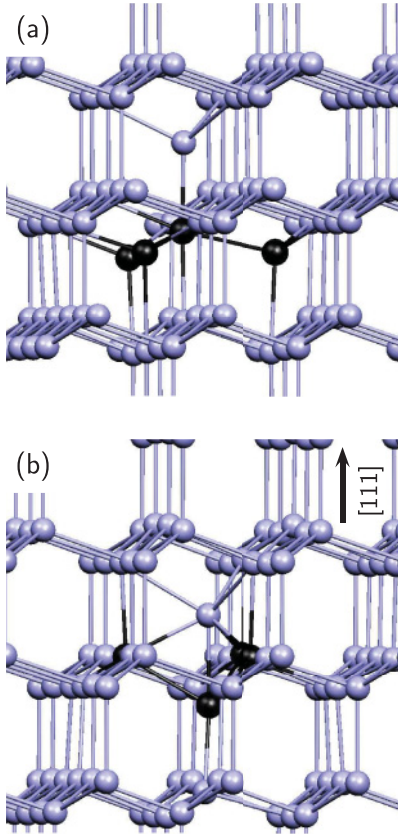


FIG. 2. (Color online) (a) The $I_{Si}Cu_5Cu_{i3}$ complex, obtained after the relaxation of Cu_{BC} with three Cu_i 's, and (b) $I_{Si}Cu_5Cu_{s3}$ complex, obtained after relaxation of $Cu_{BC}(Cu_s)_3$. In both cases, Cu_{BC} is unstable, expels a self-interstitial, and becomes substitutional. Copper atoms are represented by black spheres.

speculative arguments, notably that the Fermi level is at the right place, at least locally, or that divacancies are present in sufficient concentration.

Regardless of the assumptions involved in the formation mechanism, we analyzed the properties of $Cu_{s2}Cu_{i2}$. If we consider only the configurations where the Cu_i 's are at the nearest T site of at least one of the Cu_s , there are five possibilities. Only one of these configurations, the one depicted in Fig. 3(a), has trigonal symmetry, the (A) structure. Indeed, in Cu_{s2} , each Cu_s has two nonequivalent nearest-neighbor T sites where a Cu_i can trap, and then both Cu_i 's can also trap at the same Cu_s . The latter configuration is almost degenerate with the lowest-energy one, but does not have trigonal symmetry. The lowest-energy configuration found in this work, the (B) structure, maximizes the overlap between each Cu_i and the two Cu_s 's. In the trigonal configuration (A), the least stable of the five configurations considered and 1.01 eV higher in energy than the most stable one, each Cu_i overlaps with only one Cu_s . The most and least stable (B and A) $Cu_{s2}Cu_{i2}$ defects are shown in Fig. 3. The other three configurations have intermediate formation energies. Since Cu_i is highly mobile at room temperature and since changing one of these configurations into another involves a single hop by Cu_i , it is most likely that the only the lowest-energy structure is realized.

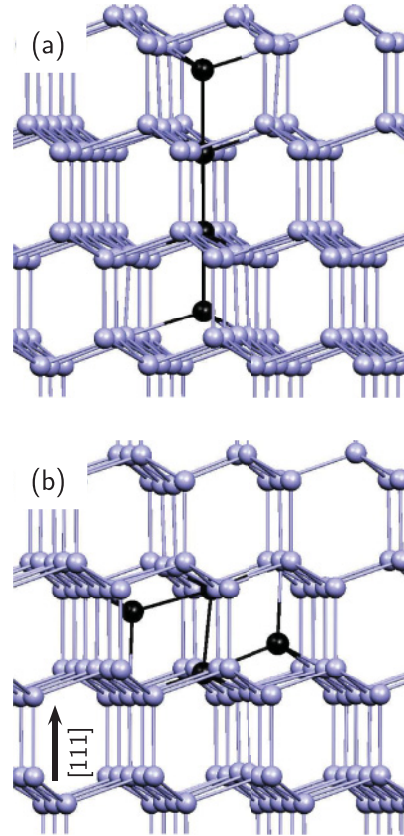


FIG. 3. (Color online) Two configurations of $Cu_{s2}Cu_{i2}$ defects. (a) Trigonal configuration (A), the highest in energy; (b) lowest-energy configuration (B). The Cu atoms are represented by black spheres.

All of the $Cu_{s2}Cu_{i2}$ defects have both donor and acceptor levels, in a close energy range: $E(0/+) = E_v + 0.40-0.45$ eV and $E(-/0) = E_c - 0.15-0.25$ eV, respectively. Thus, none of them has an electrical signature compatible with that of the Cu_{PL} defect. Further, the trigonal structure is the highest in energy. Finally, the most stable form exhibits no localized pseudolocal mode below 150 cm^{-1} . Therefore, none of the five $Cu_{s2}Cu_{i2}$ defects is a plausible candidate as Cu_{PL} .

B. $Cu_{s1}Cu_{i3}$ and Cu_{PL}

1. Properties of $Cu_{s1}Cu_{i3}$

Shirai *et al.*³² have proposed that Cu_{PL} consists of one substitutional and three interstitial copper atoms, the latter located at (or very near) any three of the four interstitial T sites adjacent to the substitutional site. This $Cu_{s1}Cu_{i3}$ defect, shown in Fig. 4, has the lowest formation energy of all the four-copper complexes considered here (Fig. 1), 0.91 eV per Cu atom, in the neutral charge state. Further, it is trigonal and should reorient easily under uniaxial stress since the activation energy for diffusion of Cu_i is very low.

The calculated $(-/0)$ level of $Cu_{s1}Cu_{i3}$ is virtually resonant with the conduction band. It is therefore very unlikely to have an acceptor level in the gap. However, it has a donor level, calculated at $E(0/+) = E_v + 0.25$ eV. The level is farther away from the valence band than the measured $E_v + 0.10$ eV (Ref. 22) donor level of Cu_{PL} , but still within the accepted

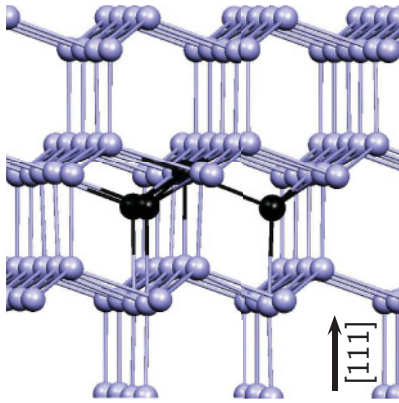


FIG. 4. (Color online) The $\text{Cu}_{s1}\text{Cu}_{i3}$ complex consists of three interstitial Cu atoms at or very near three of the four T sites adjacent to Cu_s . Copper atoms are represented by black spheres.

error bar of the marker method. The calculated vibrational spectrum of $\text{Cu}_{s1}\text{Cu}_{i3}$ shows the presence of several defect-related pseudolocal vibrational modes localized at the defect core near 90 cm^{-1} . The strongest one is an A_2 mode at 87 cm^{-1} (Fig. 5), corresponding to a twist of the three nonaxial Si atoms closest to Cu_s . The next strongest one is an E mode at $89\text{--}90\text{ cm}^{-1}$, predominantly localized on the axial Si atom.

The error bar associated with the prediction of low-frequency defect-related pLVMs is not known. In the case of high-frequency LVMs, such as Si-H stretch modes near 2000 cm^{-1} , many defects are well identified experimentally and theoretically. It is not uncommon for the predicted frequencies to be within less than 20 cm^{-1} of those measured at low temperatures, corresponding to an accuracy of about 1%. On the other hand, no pLVM has been associated with a specific defect. Further, a theoretical prediction with the same 20 cm^{-1} in the case of a pLVM at 60 cm^{-1} corresponds to a 30% error.

An additional complication arises from the fact that high-frequency LVMs are often very strongly localized at the defect. The degree of localization L_{α}^2 of a specific mode on an atom

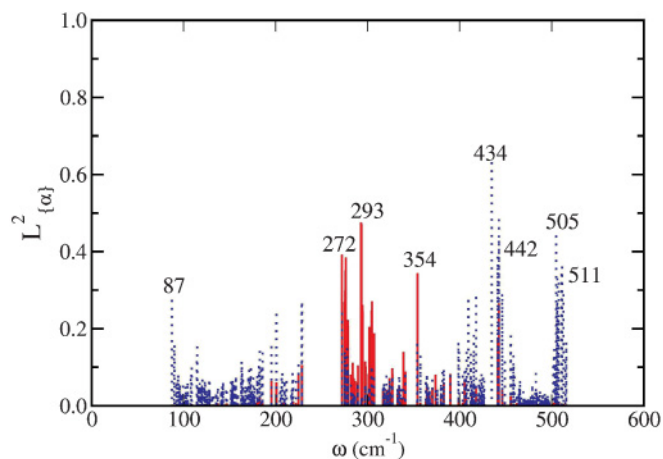


FIG. 5. (Color online) Localization L_{α}^2 of the normal vibrational modes associated with the $\text{Cu}_{s1}\text{Cu}_{i3}$ complex. The dotted (blue) lines have α running over all the Cu atoms and the solid (red) line includes the four Si atoms nearest to Cu_s .

or group of atoms α can be quantified using the eigenvectors of the dynamical matrix as discussed above (see Fig. 5). In the case of bond-centered hydrogen (H_{bc}^+), for example, L_{H}^2 for the motion of H along the trigonal axis corresponds to over 85% of the total motion of all the atoms. If one includes the two Si NNs to H, well over 90% of all the atomic displacements can be accounted for, implying that the mode is strongly localized on the defect and a few host atoms in its immediate vicinity. On the other hand, the localization of low-frequency pLVMs associated with $\text{Cu}_{s1}\text{Cu}_{i3}$ adds up to no more than 30%, indicating that many more Si atoms oscillate in this mode than in the case of H_{bc}^+ . The pLVM is much more delocalized in space, and supercell size effects could be much larger. Thus, it is much more difficult to estimate the reliability of a theoretical prediction in the case of pLVMs than of LVMs.

Additionally, the identification of phonon replicas in a PL spectrum is often tricky for a number of reasons.^{47–51} The zero-phonon line involves the recombination of an exciton, which consists of an electron state $|e\rangle$ and a hole state $|h\rangle$. The recombination involves the dipole-moment operator \hat{p} . The recombination produces the vacuum state (ground state), which transforms like the fully symmetric irreducible representation of the point group involved (A_1 in C_{3v}). Thus, the zero-phonon line is observed if the product $\Gamma_e \otimes \Gamma_p \otimes \Gamma_h$ contains A_1 , where Γ_e , Γ_p , and Γ_h are the irreducible representations of the electron state, dipole moment, and hole state, respectively. However, the local deformation of the center is driven by the properties of the bound exciton, and the symmetry of the defect in its ground state can be different from the symmetry of the exciton.^{47,48}

A phonon sideband occurs when the recombination does not produce the vacuum state but one (or more) phonons (Stokes), or when the excited state has one vibrational component (anti-Stokes). If the zero-phonon line is observed and the initial and final states are nondegenerate, then the phonon must transform like A_1 in order to be visible in the PL spectrum. But, this is not necessarily the case, as illustrated by the luminescence spectra of the vacancy in diamond, which shows phonon sidebands of E and T_1 or T_2 modes,⁴⁹ and other well-known defects in diamond, which can be found in Table I of Ref. 50. Thus, in the present situation, we can not rule out (a) that supercell size effects have an impact of the frequency and/or symmetry of the calculated pLVMs, (b) that calculations in larger supercells could show new lower-frequency normal modes, or (c) that the observed phonon sidebands have indeed a symmetry different from A_1 , as there is no experimental information on the symmetry or degeneracy of the states involved in the PL.

2. Formation of $\text{Cu}_{s1}\text{Cu}_{i3}$

A more important question relates to the fact that an entire family²⁵ of complexes involving four (sometimes five) metallic impurities is seen by PL (Cu_4 , Cu_3Ag_1 , Cu_2Ag_2 , Ag_4 , as well as centers containing Au, Li, etc.), while no complex involving two, three, or more than four (sometimes five) metals ever seems to occur. What is puzzling too is that, in the case of the four-copper defect, the most abundant and mobile species is Cu_i^+ , which should prevent aggregation because of the long-ranged Coulomb repulsion. It is important to notice that, in

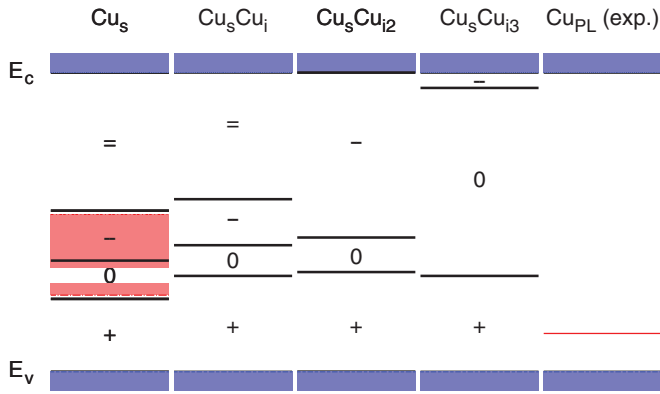
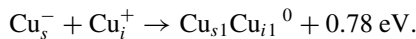


FIG. 6. (Color online) Calculated ionization levels (thick horizontal lines) for the $\text{Cu}_{s1}\text{Cu}_{in}$ complexes with $n = 0, 1, 2, 3$. The measured levels of Cu_s and Cu_{PL} (light-red shaded regions) are shown as well.

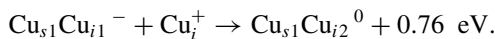
order to avoid issues associated with free-carrier absorption, all the PL experiments have been done in high-resistivity material. Therefore, we can assume that the Fermi level is near mid-gap in the samples in which Cu_{PL} has been observed.

The first step in the formation of Cu_{PL} is the existence of Cu_s . In Cu-implanted material, vacancies are created by the implantation itself. As discussed above, in situations where Cu is in-diffused at some high temperature, an anneal around 700 °C is required for Cu_{PL} to form. A small fraction of Cu_i becomes Cu_s during this anneal. We will now show that, if the Fermi level remains near mid-gap, it is plausible that the $\text{Cu}_{s1}\text{Cu}_{i3}$ defect will form. Figure 6 shows the calculated gap levels of Cu_s , $\text{Cu}_{s1}\text{Cu}_{i1}$, $\text{Cu}_{s1}\text{Cu}_{i2}$, and $\text{Cu}_{s1}\text{Cu}_{i3}$. Once Cu_s forms, it is in the single negative (-1) charge state and, therefore, traps Cu_i^+ to form the copper pair $\text{Cu}_{s1}\text{Cu}_{i1}^0$ with a gain in energy of 0.78 eV:



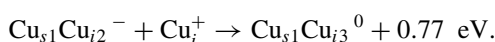
This trigonal pair has Cu_i at a T site adjacent to Cu_s .²³ Note that if one starts with two impurities A^+ and B^- , initially far apart from each other in a material with the dielectric constant of Si and places them within 2.3 Å of each other, the electrostatic energy gain is approximately 0.5 eV. Since virtually no lattice distortion is involved, the Cu_s - Cu_i binding energy is about 2/3 ionic and 1/3 covalent and the covalent overlap between Cu_i^+ and Cu_s^- leads to an energy gain of about 0.25–0.30 eV.

However, the copper pair itself has ionization levels very close to those of Cu_s . It is in the single negative (-1) charge state when the Fermi level is mid-gap. Therefore, $\text{Cu}_{s1}\text{Cu}_{i1}^0$ traps an electron, becomes $\text{Cu}_{s1}\text{Cu}_{i1}^-$, and thus becomes itself a trap for Cu_i^+ . The second Cu_i^+ traps at another T site adjacent to Cu_s :



Here, again, the binding energy is about 2/3 ionic and 1/3 covalent.

As shown in Fig. 6, $\text{Cu}_{s1}\text{Cu}_{i2}$ also has an acceptor level below mid-gap, but the double-acceptor level has been passivated. Therefore, it will trap an electron, becomes negatively charged, and trap a third Cu_i^+ :



Here, again, the binding energy is about 2/3 ionic and 1/3 covalent. But now, the calculated acceptor level $\text{Cu}_{s1}\text{Cu}_{i3}$ is almost resonant with the bottom of the conduction band, and the complex remains in the neutral charge state. The reaction stops because the trapping of an additional Cu_i^+ has no Coulombic component and would result in an energy gain of about 0.3 eV in intrinsic material, too low to be stable at room temperature. Thus, $\text{Cu}_{s1}\text{Cu}_{i4}$ will not form.

This chain of reactions resulting in the formation of $\text{Cu}_{s1}\text{Cu}_{i3}$ takes place under the experimental conditions that typically generate the Cu_{PL} defect. It would be interesting to see if similar sequences of gap levels also occur in the case of the other four- (or five-) metal complexes that have been reported. However, our argument predicts that no Cu_{PL} defect should form in p -type Si, where the Fermi level is close to the valence band. Then, even the simple Cu_sCu_i pair will not form at room temperature.

Finally, we note that there is no overlap between the three Cu_i 's in $\text{Cu}_{s1}\text{Cu}_{i3}$. The three interstitials are bound to Cu_s independently of each other, each with a binding energy of about 0.8 eV. This value is consistent with the measured 0.84 ± 0.09 eV binding enthalpy.²⁷

IV. DISCUSSION

We have calculated the properties of ten complexes containing four copper impurities in Si. The complexes studied involve various combinations of Cu_s and Cu_i . Based on the assumption that Cu_{PL} is one of the ten Cu_4 complexes we considered here, we identify plausible candidates for the Cu_{PL} defect, which is known to contain (at least) four Cu atoms. This photoluminescence center is commonly seen in high-resistivity Cu-contaminated samples and belongs to a family of a dozen four- (and sometimes five-) metal complexes.

Cu_{PL} forms following Cu implantation or Cu in-diffusion if it is followed by an ~ 700 °C anneal and a quench. The PL band consists of a zero-phonon line at 1014 meV, which correlates with a donor level at $E_v + 0.10$ eV, and phonon replicas at 57 cm^{-1} . It is trigonal, isoelectronic, and easily reorients under uniaxial stress. Its binding energy is 0.84 ± 0.09 eV. It anneals out at 250 °C, leaving isolated Cu_s . No complex containing two or three Cu atoms has been reported. Nine of the ten complexes studied can be ruled out as plausible candidates for Cu_{PL} for a variety of reasons. Some of them have an excessively large formation energy and/or the wrong symmetry and/or calculated gap levels that are incompatible with those observed and/or do not leave Cu_s following dissociation.

The Cu_4 complex with the lowest formation energy amongst those investigated is the one that has been proposed by Shirai *et al.*³² It has all the key features of Cu_{PL} , even though we have not been able to identify the specific pLVM responsible for the observed phonon sidebands. The most interesting feature of this defect is that it must form in intrinsic and n -type Si as soon as Cu_s forms. The key lies in the position of the donor and especially acceptor levels of the $\text{Cu}_{s1}\text{Cu}_{in}$ series of complexes. Indeed, if $n = 0$, Cu_s is in the single negative (-1) charge state in intrinsic Si and therefore traps Cu_i^+ to form $\text{Cu}_{s1}\text{Cu}_{i1}$. This pair is also in the single negative charge state in intrinsic Si

and traps an additional Cu_i^+ to form $\text{Cu}_{s_1}\text{Cu}_{i_2}$. This complex also has an acceptor level below mid-gap and, therefore, traps another Cu_i^+ to form $\text{Cu}_{s_1}\text{Cu}_{i_3}$. But, the sequence of events stops there as the acceptor level of $\text{Cu}_{s_1}\text{Cu}_{i_3}$ is resonant with the conduction band. As a result, the only complex in the entire series is $\text{Cu}_{s_1}\text{Cu}_{i_3}$. At each step, the binding energy of Cu_i is about 0.8 eV.

It is tempting to speculate that a similar coincidence of gap levels is the reason for the formation of the other four- (or five-) metal complexes that have been reported in the PL studies. Future theoretical studies are needed to confirm this.

ACKNOWLEDGMENTS

We are most thankful to G. Davies for numerous discussions regarding photoluminescence, phonon sidebands, and bound excitons. The work of A.C. is supported by Marie-Curie SiNanoTune program, and was in part carried out in Milipeia (University of Coimbra). The work of S.K.E. is supported in part by the Grant No. D-1126 from the R.A. Welch Foundation and a contract from the Silicon Solar Consortium. Many thanks to Texas Tech's High Performance Computing Center for generous amounts of CPU time.

*aicarvalho@ua.pt

- ¹A. A. Istratov, T. Buonassisi, R. J. McDonald, A. R. Smith, R. Schindler, J. A. Rand, J. P. Kalejs, and E. R. Weber, *J. Appl. Phys.* **94**, 6552 (2003).
- ²T. Buonassisi, A. A. Istratov, M. A. Marcus, B. Lai, Z. Cai, S. M. Heald, and E. R. Weber, *Nat. Mater.* **4**, 676 (2005).
- ³H. Lemke, *Phys. Status Solidi A* **95**, 665 (1986).
- ⁴A. A. Istratov, H. Hieslmair, C. Flink, and E. R. Weber, *Appl. Phys. Lett.* **71**, 2349 (1997).
- ⁵A. A. Istratov, C. Flink, H. Hieslmair, E. R. Weber, and T. Heiser, *Phys. Rev. Lett.* **81**, 1243 (1998).
- ⁶D. J. Backlund and S. K. Estreicher, *Phys. Rev. B* **81**, 235213 (2010).
- ⁷Y. Kamon, H. Harima, A. Yanase, and H. Katayama-Yoshida, *Phys. B (Amsterdam)* **308–310**, 391 (2001).
- ⁸A. A. Istratov, T. Buonassisi, M. D. Pickett, M. Heuera, and E. R. Weber, *Mater. Sci. Eng. B* **134**, 282 (2006).
- ⁹H. Savin, M. Yli-Koski, and A. Haarahiltunen, *Appl. Phys. Lett.* **95**, 152111 (2009).
- ¹⁰A. A. Istratov, C. Flink, H. Hieslmair, T. Heiser, and E. R. Weber, *Appl. Phys. Lett.* **71**, 2121 (1997).
- ¹¹M. Seibt, H. Hedemann, A. A. Istratov, F. Riedel, A. Sattler, and W. Schröter, *Phys. Status Solidi A* **171**, 301 (1999).
- ¹²T. Buonassisi, A. A. Istratov, M. D. Pickett, M. A. Marcus, T. F. Cizzek, and E. R. Weber, *Appl. Phys. Lett.* **89**, 042102 (2006).
- ¹³W. Wang, D. Yang, X. Ma, and D. Que, *J. Appl. Phys.* **103**, 093534 (2008).
- ¹⁴S. D. Brotherton, J. R. Ayres, A. Gill, H. W. van Kesteren, and F. J. M. Greidanus, *J. Appl. Phys.* **62**, 1286 (1987).
- ¹⁵S. Knack, J. Weber, and H. Lemke, *Phys. B (Amsterdam)* **273–274**, 387 (1999).
- ¹⁶S. Knack, J. Weber, H. Lemke, and H. Riemann, *Phys. Rev. B* **65**, 165203 (2002).
- ¹⁷A. A. Istratov and E. R. Weber, *Appl. Phys. A* **66**, 123 (1998).
- ¹⁸N. Yarykin and J. Weber, *Phys. Rev. B* **83**, 125207 (2011).
- ¹⁹J. Weber, H. Bauch, and R. Sauer, *Phys. Rev. B* **25**, 7688 (1982).
- ²⁰N. S. Minaev, A. V. Mudryi, and V. D. Tkachev, *Fiz. Tekh. Poluprovodn.* **13**, 395 (1979) [*Sov. Phys. Semicond.* **13**, 233 (1979)].
- ²¹E. R. Weber, *Appl. Phys. A* **30**, 1 (1983).
- ²²H. B. Erzgräber and K. Schmalz, *J. Appl. Phys.* **78**, 4066 (1995).
- ²³S. K. Estreicher, D. West, J. Goss, S. Knack, and J. Weber, *Phys. Rev. Lett.* **90**, 035504 (2003).
- ²⁴J. E. Lowther, *Mater. Sci. Semicond. Process.* **13**, 29 (2010).
- ²⁵M. Steger, A. Yang, N. Stavrias, M. L. W. Thewalt, H. Riemann, N. V. Abrosimov, M. F. Churbanov, A. V. Gusev, A. D. Bulanov, I. D. Kovalev, A. K. Kaliteevskii, O. N. Godisov, P. Becker, and H.-J. Pohl, *Phys. Rev. Lett.* **100**, 177402 (2008).
- ²⁶M. Steger, A. Yang, T. Sekiguchi, K. Saedi, M. L. W. Thewalt, M. O. Henry, K. Johnston, H. Riemann, N. V. Abrosimov, M. F. Churbanov, A. V. Gusev, A. K. Kaliteevskii, O. N. Godisov, P. Becker, and H.-J. Pohl, *J. Appl. Phys.* (in print).
- ²⁷A. A. Istratov, H. Hieslmair, T. Heiser, C. Flink, and E. R. Weber, *Appl. Phys. Lett.* **72**, 474 (1998).
- ²⁸M. Nakamura and H. Iwasaki, *J. Appl. Phys.* **86**, 537 (1999).
- ²⁹M. Nakamura, S. Murakami, N. J. Kawai, S. Saito, K. Matsukawa, and H. Arie, *Jpn. J. Appl. Phys.* **48**, 082302 (2009).
- ³⁰S. Knack, J. Weber, H. Lemke, and H. Riemann, *Phys. B (Amsterdam)* **308–310**, 404 (2001).
- ³¹S. Knack, *Mater. Sci. Semicond. Process.* **7**, 125 (2004).
- ³²K. Shirai, H. Yamaguchi, A. Yanase, and H. Katayama-Yoshida, *J. Phys. Condens. Matter* **21**, 064249 (2009).
- ³³M. Nakamura and S. Murakami, *Jpn. J. Appl. Phys.* **49**, 071302 (2010).
- ³⁴M. Nakamura, S. Ishiwari, and A. Tanaka, *Appl. Phys. Lett.* **73**, 2325 (1998).
- ³⁵M. Nakamura, S. Murakami, N. J. Kawai, S. Saito, and H. Arie, *Jpn. J. Appl. Phys.* **47**, 4398 (2008).
- ³⁶N. Troullier and J. L. Martins, *Phys. Rev. B* **43**, 1993 (1991).
- ³⁷L. Kleinman and D. M. Bylander, *Phys. Rev. Lett.* **48**, 1425 (1982).
- ³⁸P. Hohenberg and W. Kohn, *Phys. Rev.* **136**, B864 (1964); W. Kohn and L. J. Sham, *ibid.* **140**, A1133 (1965).
- ³⁹D. Sánchez-Portal, P. Ordejón, E. Artacho, and J. M. Soler, *Int. J. Quantum Chem.* **65**, 453 (1997).
- ⁴⁰E. Artacho, D. Sánchez-Portal, P. Ordejón, A. García, and J. M. Soler, *Phys. Status Solidi B* **215**, 809 (1999).
- ⁴¹J. P. Perdew, K. Burke, and M. Ernzerhof, *Phys. Rev. Lett.* **77**, 3865 (1996).
- ⁴²O. F. Sankey and D. J. Niklewski, *Phys. Rev. B* **40**, 3979 (1989).
- ⁴³O. F. Sankey, D. J. Niklewski, D. A. Drabold, and J. D. Dow, *Phys. Rev. B* **41**, 12750 (1990).
- ⁴⁴H. J. Monkhorst and J. D. Pack, *Phys. Rev. B* **13**, 5188 (1976).
- ⁴⁵J. Coutinho, V. J. B. Torres, R. Jones, and P. R. Briddon, *Phys. Rev. B* **67**, 035205 (2003).
- ⁴⁶D. J. Backlund and S. K. Estreicher (unpublished).
- ⁴⁷G. Davies, M. Zafar Iqbal, and E. C. Lightowlers, *Phys. Rev. B* **50**, 11520 (1994).
- ⁴⁸G. Davies, *Phys. Rev. B* **51**, 13783 (1995).
- ⁴⁹G. Davies, *J. Phys. C: Solid State Phys.* **15**, L149 (1982).
- ⁵⁰G. Davies, *Rep. Prog. Phys.* **44**, 787 (1981).
- ⁵¹G. Davies (private communication).